

Toward high-dimensional-state quantum memory in a cold atomic ensembleDong-Sheng Ding,^{1,2} Wei Zhang,^{1,2} Zhi-Yuan Zhou,^{1,2} Shuai Shi,^{1,2} Jian-song Pan,^{1,2} Guo-Yong Xiang,^{1,2} Xi-Shi Wang,³ Yun-Kun Jiang,⁴ Bao-Sen Shi,^{1,2,*} and Guang-Can Guo^{1,2}¹Key Laboratory of Quantum Information, University of Science and Technology of China, Hefei 230026, China²Synergetic Innovation Center of Quantum Information & Quantum Physics, University of Science and Technology of China, Hefei, Anhui 230026, China³State Key Laboratory of Fire Science, University of Science & Technology of China, Hefei, Anhui 230026, China⁴College of Physics and Information Engineering, Fuzhou University, Fuzhou, 350002, China

(Received 12 December 2013; published 1 October 2014)

Quantum memories have been realized in different physical systems, such as atomic ensembles or solid systems. To date, all quantum memories have realized the storage and retrieval of photons encoded using only a two-dimensional space spanned, for example, by the orthogonal polarization states, and hence can only store a quantum bit. Using electromagnetically induced transparency in a cold atomic ensemble, we report the experimental realization of a quantum memory storing a photon encoded in a three-dimensional space spanned by orbital angular momentum (OAM) states. We experimentally reconstruct the storage process density matrix with a fidelity of $85.3\% \pm 1.8\%$ using a 4-f imaging system. We also realize storage of two special photonic qutrit states as examples. Toward storing a higher-dimensional state encoded in OAM space, the efficiency difference between different OAM states should be considered according to the experimental results. The capability to store high-dimensional quantum states with high fidelity is a key step towards building high-dimensional quantum networks.

DOI: [10.1103/PhysRevA.90.042301](https://doi.org/10.1103/PhysRevA.90.042301)

PACS number(s): 03.67.Lx, 42.50.Gy, 42.65.Hw

I. INTRODUCTION

The reversible transfer of quantum information between a photon, an information carrier, and a quantum memory with high fidelity and reliability is the prerequisite for realizing a long-distance quantum communication and a quantum network [1,2]. Usually quantum information is encoded using a two-dimensional space spanned, for example, by the orthogonal polarization states of a photon or the different paths along which a photon propagates. In this way, each photon could carry a quantum bit (qubit) of information. If the photon could be encoded in a high-dimensional space, for example, spanned by the inherently infinite-dimensional orbital angular momentum (OAM) states, then the information carried by each photon could be increased significantly [from a qubit to \log_2^d bits (hereafter called a qudit), where d is the number of orthogonal basis vectors of the Hilbert space in which the photon is described], and the channel capacity of the network and the transmission efficiency could also be greatly improved [3,4]. Moreover, in comparison with a two-dimensional state, high-dimensional states show many interesting properties; they make more efficient quantum-information processing possible and afford a more secure flux of information in quantum key distributions [5]. Therefore quantum communication research based on a carrier encoded using a high-dimensional space has become a hot topic and has attracted much attention recently. Some quantum schemes using, for example, a photonic high-dimensional time-bin state [6] or an OAM state [7,8] have been reported. Quantum repeaters are indispensable for increasing transmission distances and improving quantum-information processing efficiency [9]. A quantum memory is the key component of quantum repeaters. If we could realize

the reversible transfer of a high-dimensional quantum state between a true single photon and matter (for example, an atomic ensemble or a solid system) used as a quantum memory with high fidelity and reliability, then we may enhance the channel capacity significantly. Furthermore, it could overcome distance limitations of quantum communication schemes through transmission losses that a high-dimensional quantum network may be expected to have. Moreover, a quantum memory for storing a high-dimensional state can reduce its sensitivity to memory coherence time [10]. It can lead to significant improvements in storage capacity [11], and could potentially find some novel quantum-information applications such as quantum holographic teleportation [12], quantum dense image coding [13], and holographic quantum computing [14]. After the seeding work of storing a light-carrying OAM in an atomic ensemble was reported by Moretti *et al.* in Ref. [15], many groups and researchers are active in storing light encoded using a high-dimensional space. Although some work has been reported for light-carrying OAM or spatial structures in different physical systems, such works involve intense light sources [16–23]. Very recently, Refs. [24] and [25] reported on the storage of light at the single-photon level, imprinted with an OAM state; however, the photon was still encoded in a two-dimensional space, carrying a qubit of information. To date, there has been no work reporting on the storage of a photon encoded in a high-dimensional state in any physical system. How to construct such a quantum memory has been a big challenge. Here we report on the experimental realization of a quantum memory that stores true single photons encoded with a high-dimensional quantum state.

This stored single photon is a heralded single photon prepared through the spontaneous four-wave mixing (SFWM) process via a double- Λ configuration in a cold atomic ensemble. It carried an OAM imprinted through a spatial light modulator (SLM) and is stored in another cold atomic

*drshi@ustc.edu.cn

ensemble acting as a quantum memory via electromagnetically induced transparency (EIT). We reconstructed the storage process density matrix of a three-dimensional state (qutrit) by quantum process tomography with a fidelity of $85.3\% \pm 1.8\%$ using a 4-f imaging system, proving the feasibility of storing a qutrit in this kind of memory. Furthermore, as examples, we realized the experimental storage of two special photonic qutrit states. We also found the storage efficiencies are different for the different OAM states, which should be considered for realizing higher-dimensional-state quantum memory. Our results show that there exists a quantum memory for a photonic qudit and it makes a significant step toward the realization of a high-dimensional quantum memory in the future.

II. EXPERIMENTAL SETUP

We prepared the single photon for the storage via SFWM in a cold Rb 85 atomic ensemble trapped in a two-dimensional magneto-optical trap (MOT) [26]. The experimental setup shown in Fig. 1(a) is the same as Ref. [25]. The optical depth measured for MOT 1 was about 8. The photon signal 1 at 780 nm and photon signal 2 at 795 nm were respectively called the trigger and the signal hereafter, and the signal was stored for subsequent treatment. The laser power of pumps 1 and 2 were 660 and 45 μW , respectively. We characterized the nonclassical correlation between photon pairs and the

single-photon property of the signal photon using the method and procedure presented in Ref. [25]. The experimental storage of the signal through EIT was implemented in MOT 2. The optical depth of MOT 2 was about 20. The bandwidth for storage was about 30 MHz. The Rabi frequency of the coupling laser was 4Γ , where Γ is the decay rate of level $|4\rangle$, and the beam waist of this parallel light was 2.5 mm. The waist of signal at the surface of the SLMs was 2.5 mm (the same as at the fiber coupler) and was 30 μm at MOT 2. Figure 1(b) showed the time-correlated function between the input signal and the trigger, and Fig. 1(c) corresponded to the correlated function between the retrieved signal and the trigger after a programmed storage time. We further obtained an α value of 0.006 for the signal before storage and 0.08 for the retrieved signal from MOT 2. Here, the anticorrelation parameter α was calculated by α ($\alpha = \frac{P_{12}P_{13}}{P_{123}}$), where P_1 indicates the trigger photon counts, P_{12} and P_{13} are the twofold coincidence counts between the trigger and the two separated signal photons by a beam splitter, and P_{123} corresponds to threefold coincidence counts. Both α values go to zero, clearly confirming that the single-photon nature is preserved during storage.

III. EXPERIMENTAL RESULTS

The storage and later release of an input state can be considered as a state transfer process and is represented by a quantum process density matrix χ . The main focus here is to reconstruct this matrix. We take the storage of a qutrit state as an example. This photonic qutrit is encoded using a space spanned by the OAM states. To reconstruct the density matrix χ , we performed quantum process tomography. The output state can be written as $\varepsilon(\rho) = \sum_{m,n=1}^9 \chi_{mn} \hat{\lambda}_m \rho \hat{\lambda}_n^\dagger$, where $\hat{\lambda}_m, \hat{\lambda}_n^\dagger$ is an operator acting on the input state ρ . The matrix χ can be obtained by measuring the output state $\varepsilon(\rho)$; the complete operator set for reconstructing χ for storing the photonic qutrit could be referenced in Ref. [27]. The input states could be chosen from a single OAM state or an OAM superposition state $|\psi_{1-9}\rangle$ corresponding to the states $|L\rangle, |G\rangle, |R\rangle, (|G\rangle + |L\rangle)/\sqrt{2}, (|G\rangle + |R\rangle)/\sqrt{2}, (|G\rangle + i|L\rangle)/\sqrt{2}, (|G\rangle - i|R\rangle)/\sqrt{2}, (|L\rangle + |R\rangle)/\sqrt{2}$, and $(|L\rangle + i|R\rangle)/\sqrt{2}$. It is worth pointing out that these states only contain the single-eigenstate OAM mode or the two-OAM superposition state, which means we could store two OAM modes every time at most. For that, we input one of nine different states $|\psi_{1-9}\rangle$ to MOT 2 for storage, respectively, where $|L\rangle, |G\rangle$, and $|R\rangle$ are states corresponding to a well-defined OAM of $1\hbar, 0$ and $-1\hbar$, respectively. These input states, having different phases and intensity distributions [see Fig. 2(a)], were prepared through SLM1 (HOLOEYE, PLUTO, an active area of 15.36×8.64 mm, the pixel pitch size is 8 μm , and the total pixels are 1920×1080). The SLM is of reflective type with a 60% efficiency. After the programmed storage time, the stored state was retrieved and measured in nine different OAM basis vectors, the same as the nine input states [28]. These basis vectors for measurements were prepared by another spatial light modulator (SLM 2) and set to be in reversible phase rotations compared with the corresponding input states to obtain a Gaussian mode for measurement.

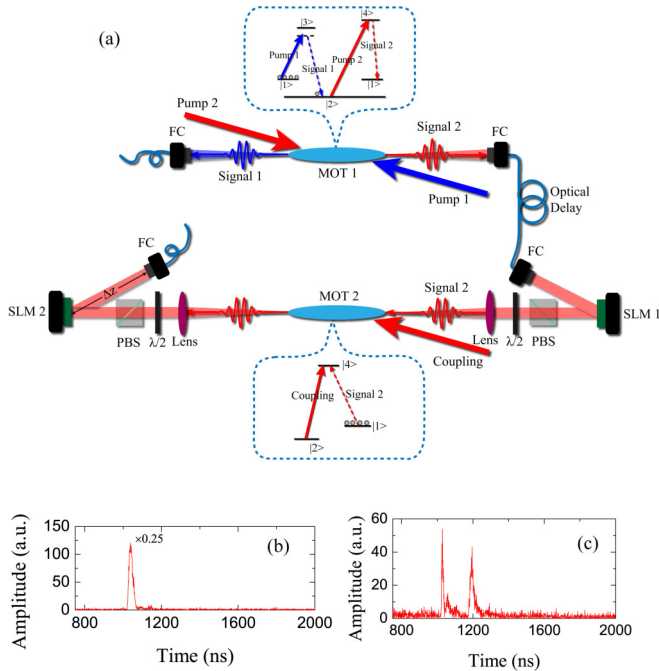


FIG. 1. (Color online) Simplified experimental setup. (a) Schematic diagram depicting the generation of nonclassical photon pairs using SFWM and the storage of a single photon encoded as a high-dimensional state. MOT: magneto-optical trap; lens: lens with focus length of 500 mm; FC: fiber coupler; SLM: spatial light modulator; PBS: polarization beam splitter; $\lambda/2$: half-wave plate. Inset: energy-level diagrams for SFWM and EIT, respectively. (b) Cross correlation between the input signal and the trigger. The data were scaled by 0.25. (c) Cross-correlation function between the retrieved signal and the trigger after a programmed storage time. (b) and (c) are obtained without both SLMs.

In addition, the 4-f imaging system used was the key in correctly reconstructing the density matrix. The system comprised SLM 1 acting as a mask plane, the center of the atomic ensemble in MOT 2 was the Fourier plane, and SLM 2 represented the image plane; two lenses with focal length of 500 mm were used to image SLM 1 onto SLM 2. Because of conjugate properties between the mask plane and the image plane, the vectors for measurements need to be converted to the conjugates of the corresponding input states. Furthermore, we note that the stored image in the atomic ensemble is the Fourier transformation of the input phase structure; the phase distributions at the image plane or the measurement plane were the Fourier transformations of the OAM states. Hence, in order to collect the retrieved OAM state of the input photon correctly, we set the single-mode fiber coupler to be 2.5 m away from the SLM 2 [Fig. 1(a)], by which the spatial structured mode at far-field diffraction could be easily collected by the single-mode fiber. In this process, Fresnel diffraction can be ignored and Fraunhofer diffraction dominates. By inputting nine input states, measuring each retrieved input state in the nine basis vectors, and then integrating coincidence counts in a 50-ns coincidence window with background noise subtracted in each measurement (the background noise is the coincidence count with no input photon for storage in MOT 2), we obtained a set of 81 data points and reconstructed the quantum process density matrix for our quantum memory system using these data, referenced as the method in [27,29]. The results are shown in Figs. 2(b) and 2(c), where (b) gives the real part of the density matrix and

(c) the corresponding imaginary part. Compared with the ideal quantum storage process density matrix, the fidelity obtained for our density matrix was $85.3\% \pm 1.8\%$ by using a formula $F = \text{Tr}(\sqrt{\sqrt{\chi} \chi_{\text{ideal}} \sqrt{\chi}})^2$. (The error bar of our experimental measurement was estimated from Poissonian statistics and using Monte Carlo simulations.)

By reconstructing the quantum storage process density matrix, we conclude that our system can store a photonic qutrit. To further illustrate this storage capability, we performed experiments where we stored two special photonic qutrits $|\Psi_1\rangle = (|L\rangle + |G\rangle + |R\rangle)/\sqrt{3}$ and $|\Psi_2\rangle = (|L\rangle - |G\rangle + |R\rangle)/\sqrt{3}$ as examples. The phase structures and the intensity distributions of these two states are given in Figs. 3(a) and 3(d). By projecting these two states on the nine basis vectors defined before, we obtained the corresponding nine coincidence counts and used them to reconstruct the density matrix of the retrieved state, shown in Fig. 3(b), 3(c), 3(e), and 3(f), where 3(b) and 3(e) are the real parts of the retrieved photonic qutrit states and 3(c) and 3(f) the corresponding imaginary parts. We calculated the fidelities of the reconstructed density matrices by comparing them with the ideal density matrices, obtaining $77\% \pm 3\%$ for state $|\Psi_1\rangle$ and $80\% \pm 2\%$ for state $|\Psi_2\rangle$.

The fidelity of the storage process is below 100%, and we believe the main reasons are as follows: (1) In the experiment, we used a 4-f imaging for measuring the retrieved state. The mismatch between the actual position of the signal beam in fact produces exposures at the SLM2 and the ideal position the signal should produce exposures reduces the fidelity. One could soften this influence by enlarging the beam waist of the signal. (2) When the input state is $|\psi_8\rangle$ or $|\psi_9\rangle$, or the projection of any input state in the basis vector of $|\psi_8\rangle$ or $|\psi_9\rangle$, the relative short distance of 2.5 m might not completely project the input state into the Gaussian mode, thus inducing errors and reducing fidelity. For the same reasons, the fidelity of the photonic qutrit states used as examples is affected more significantly, because a three-dimensional state prepared by SLM is used as an input in these cases compared with process density matrix reconstruction where a two-dimensional state is used.

For realizing the quantum communication based on high-dimensional encoding, in the future a quantum memory which could store a higher-dimensional quantum state is needed. Such a memory could also be checked by using the storage process tomography as used before. In such a process, the storage of a photon carrying a single-eigenstate OAM mode $|\Psi_l\rangle$ or a photon carrying the superposition of two OAMs $|\Psi_{l1}\rangle + e^{i\theta}|\Psi_{l2}\rangle$ is performed (where $l, l1$, and $l2$ are the quanta of OAM mode), and then a storage process matrix could be reconstructed. So here we check the storage of a single-eigenstate OAM or an OAM-superposition-carrying photon. In order to simplify the experiment, we use the weak coherent light as the input signal instead; the input signal and retrieved signal are recorded by a high-resolution camera (1024×1024 , iStar 334T series, Andor), which worked at a single-photon level. Through recoding input and the retrieved intensity of different OAMs, we calculate the memory efficiency. The results are given in Fig. 4. The efficiency of memory decreases along with the increment of OAM quanta. This result gives us a hint that such a state $|\Psi_{l1}\rangle + e^{i\theta}|\Psi_{l2}\rangle$ with large difference quanta of $l1$ and $l2$ might be distorted during quantum memory due to unbalanced efficiency. At the center of the atomic

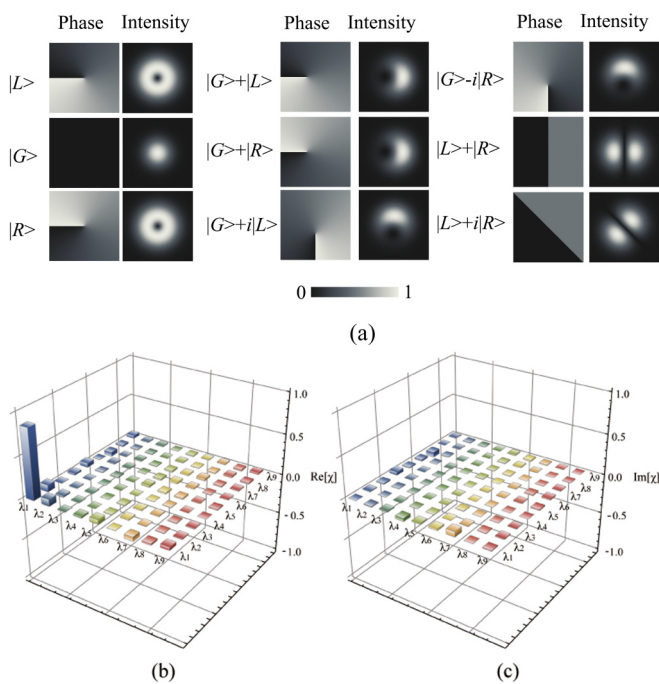


FIG. 2. (Color online) Reconstructing quantum storage process density matrix. (a) The intensity (right panel of each pair) and the phase (left panel) distributions of the input OAM states. (b) and (c) are the real and imaginary parts of the reconstructed quantum storage process density matrix. λ_{1-9} is a basis set for operators defined in the Supplemental Material [30].

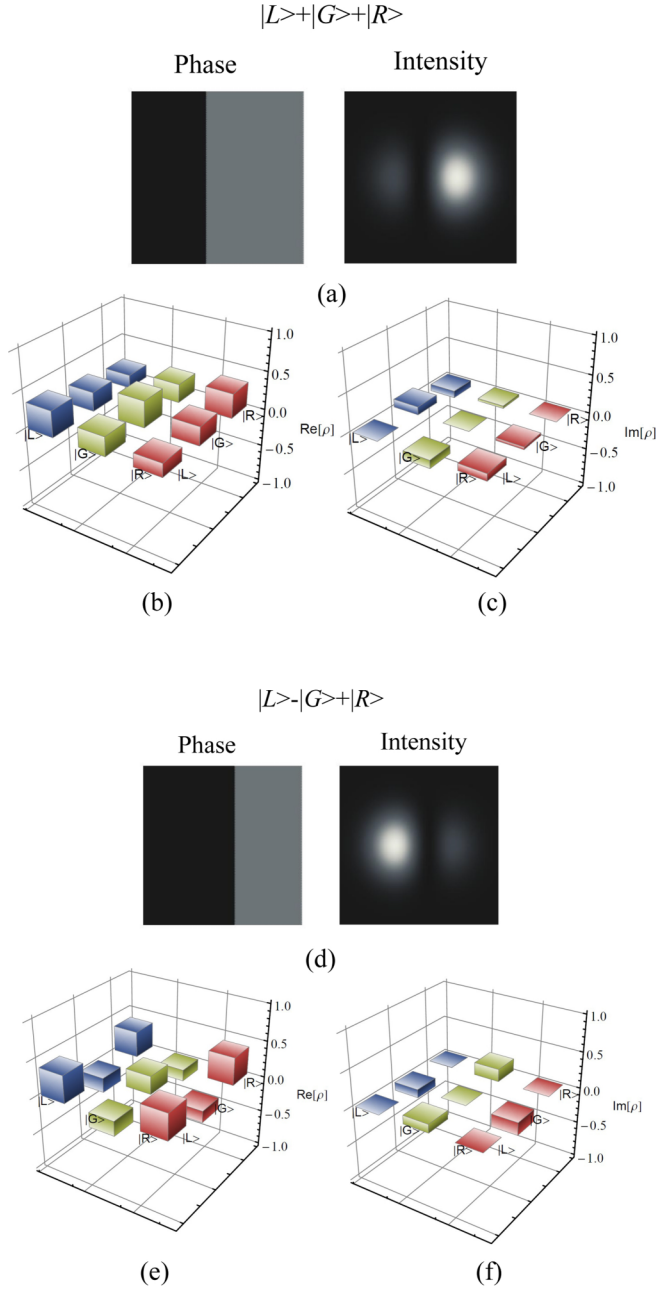


FIG. 3. (Color online) Storing photonic qutrits. (a) The phase (left panel of each pair) and the intensity (right panel) distributions of the photonic qutrit state $|\Psi_1\rangle$. (b) and (c) are the real and imaginary parts of the reconstructed density matrix of the retrieved photonic qutrit $|\Psi_1\rangle$. (d), (e), and (f) are similar to (a), (b), and (c) but for the photonic qutrit state $|\Psi_2\rangle$.

ensemble, the OAM mode with quanta of l has a waist of $w(z) = \sqrt{l+1}w_0(z)$, where $w_0(z)$ is the beam waist of a Gaussian light. Thus there is a large difference in storage efficiency due to the different beam waists among the small quanta OAM modes. Instead, at high quanta OAM modes, there is little difference between the beam waists, thus resulting in a small difference in efficiency. The second thing is that we need to know whether the relative phase θ between $|\Psi_{l1}\rangle$ and $|\Psi_{l2}\rangle$ changes or not during the storage. In the EIT quantum

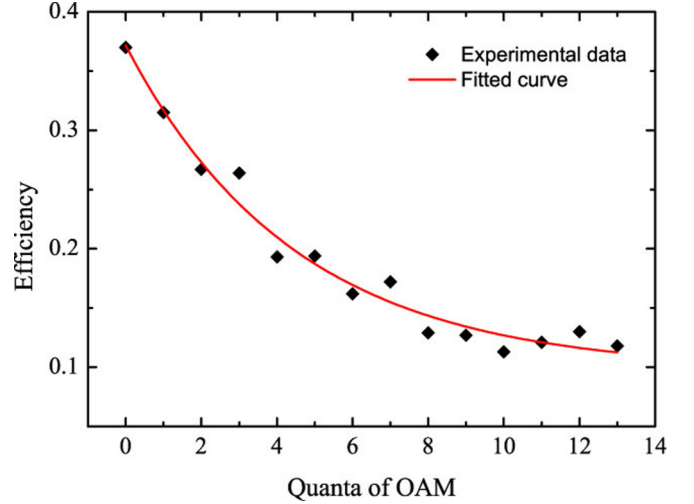


FIG. 4. (Color online) The efficiency of quantum memory of different OAM states. The blue solid line is the fitted curve by a formula $y = Ae^{-x/T} + y_0$, where $A = 0.27$, $T = 4.4$, and $y_0 = 0.01$.

memory scheme, the frequency of the photonic state $|\Psi_{l1}\rangle$ and $|\Psi_{l2}\rangle$ is the same; the relative phase does not change due to the same evolution of $|\Psi_{l1}\rangle$ and $|\Psi_{l2}\rangle$, memorized as atomic spin waves when the angle between the coupling and signal beams is much greater than the direction angle of the signal beam.

IV. CONCLUSION

In conclusion, we have reported on the experimental realization of a quantum memory storing a true single photon encoded with a high-dimensional quantum state, and experimentally gave the boundedness of our quantum memory device for storing the high-dimensional state with large quanta of OAM, which is the different ratio of memory efficiency of different OAM states. Although our work provides a proof of principle of storing a photonic qutrit, it is the first step towards realizing a high-dimensional quantum memory. Moreover, for extension to the reconstruction of quantum process density matrices corresponding to high-dimensional OAM states ($d \geq 4$) in accordance with Ref. [29], many experimental parameters should be considered: (1) The big challenge we face in the experimental demonstrations is further improvements in technique, such as how to achieve a higher signal-to-noise ratio and how to stabilize the system over long periods. This is because we will have to take more data. (2) We must achieve the same efficiency of different OAM states in the process of storing high-dimensional states in the future. (3) Reference [31] states that the number of dimensions per photon in practice was limited by several factors, such as the Fresnel number and the optical depth of the atomic ensemble, the angle of the signal field and the control field, etc. The requires further investigation.

ACKNOWLEDGMENTS

We thank Dr. Xian-Min Jin, Dr. Xi-Feng Ren, and Dr. Jin-Shi Xu for helpful discussions. This work was supported by the National Fundamental Research Program of China (Grant No. 2011CBA00200), the National Natural

Science Foundation of China (Grants No. 11174271, No. 61275115, and No. 61435011), the Youth Innovation Fund

from USTC (Grant No. ZC 9850320804), and the Innovation Fund from the CAS, a program of the NCET.

-
- [1] A. Lvovsky, B. C. Sanders, and W. Tittel, *Nature Photon.* **3**, 706 (2009).
- [2] H. J. Kimble, *Nature (London)* **453**, 1023 (2008).
- [3] A. Mair, A. Vaziri, G. Weihs, and A. Zeilinger, *Nature (London)* **412**, 313 (2001).
- [4] J. Leach, B. Jack, J. Romero, A. K. Jha, A. M. Yao, S. Franke-Arnold, D. G. Ireland, R. W. Boyd, S. M. Barnett, and M. J. Padgett, *Science* **329**, 662 (2010).
- [5] H. Bechmann-Pasquinucci and W. Tittel, *Phys. Rev. A* **61**, 062308 (2000).
- [6] H. De Riedmatten, I. Marcikic, H. Zbinden, and N. Gisin, *Quantum Inf. Comput.* **2**, 425 (2002).
- [7] R. Fickler, R. Lapkiewicz, W. N. Plick, M. Krenn, C. Schaeff, S. Ramelow, and A. Zeilinger, *Science* **338**, 640 (2012).
- [8] A. C. Dada, J. Leach, G. S. Buller, M. J. Padgett, and E. Andersson, *Nat. Phys.* **7**, 677 (2011).
- [9] H.-J. Briegel, W. Dur, J. I. Cirac, and P. Zoller, *Phys. Rev. Lett.* **81**, 5932 (1998).
- [10] O. A. Collins, S. D. Jenkins, A. Kuzmich, and T. A. B. Kennedy, *Phys. Rev. Lett.* **98**, 060502 (2007).
- [11] C. Simon, H. de Riedmatten, M. Afzelius, N. Sangouard, H. Zbinden, and N. Gisin, *Phys. Rev. Lett.* **98**, 190503 (2007).
- [12] I. V. Sokolov, M. I. Kolohov, A. Gatti, and L. A. Lugiato, *Opt. Commun.* **193**, 175 (2001).
- [13] T. Y. Golubeva, Y. Golubev, I. V. Sokolov, and M. I. Kolobov, *J. Mod. Opt.* **53**, 699 (2006).
- [14] K. Tordrup, A. Negretti, and K. Molmer, *Phys. Rev. Lett.* **101**, 040501 (2008).
- [15] D. Moretti, D. Felinto, and J. W. R. Tabosa, *Phys. Rev. A* **79**, 023825 (2009).
- [16] P. K. Vudyasetu, R. M. Camacho, and J. C. Howell, *Phys. Rev. Lett.* **100**, 123903 (2008).
- [17] M. Shuker, O. Firstenberg, R. Pugatch, A. Ron, and N. Davidson, *Phys. Rev. Lett.* **100**, 223601 (2008).
- [18] J. H. Wu, Y. Liu, D. S. Ding, Z. Y. Zhou, B. S. Shi, and G. C. Guo, *Phys. Rev. A* **87**, 013845 (2013).
- [19] D. S. Ding, J. H. Wu, Z. Y. Zhou, B. S. Shi, X. B. Zou, and G. C. Guo, *Phys. Rev. A* **87**, 053830 (2013).
- [20] G. Heinze, A. Rudolf, F. Beil, and T. Halfmann, *Phys. Rev. A* **81**, 011401(R) (2010).
- [21] M. Hosseini, B. M. Sparkes, G. Campbell, P. K. Lam, and B. C. Buchler, *Nat. Commun.* **2**, 174 (2011).
- [22] D. B. Higginbottom, B. M. Sparkes, M. Rancic, O. Pinel, M. Hosseini, P. K. Lam, and B. C. Buchler, *Phys. Rev. A* **86**, 023801 (2012).
- [23] Q. Glorieux, J. B. Clark, A. M. Marino, Z. F. Zhou, and P. D. Lett, *Opt. Express* **20**, 12350 (2012).
- [24] A. Nicolas, L. Veissier, L. Giner, E. Giacobino, D. Maxein, and J. Laurat, *Nat. Photonics* **8**, 234 (2014).
- [25] D.-S. Ding, Z.-Y. Zhou, B.-S. Shi, and G.-C. Guo, *Nat. Commun.* **4**, 2527 (2013).
- [26] Y. Liu, J.-H. Wu, B.-S. Shi, and G.-C. Guo, *Chin. Phys. Lett.* **29**, 024205 (2012).
- [27] R. T. Thew, K. Nemoto, A. G. White, and W. J. Munro, *Phys. Rev. A* **66**, 012303 (2002).
- [28] R. Inoue, T. Yonehara, Y. Miyamoto, M. Koashi, and M. Kozuma, *Phys. Rev. Lett.* **103**, 110503 (2009).
- [29] I. L. Chuang and M. A. Nielsen, *J. Mod. Opt.* **44**, 2455 (1997).
- [30] See Supplemental Material at <http://link.aps.org/supplemental/10.1103/PhysRevA.90.042301> for Qutrit tomography and image projection.
- [31] A. Grodecka-Grad, E. Zeuthen, and A. S. Sorensen, *Phys. Rev. Lett.* **109**, 133601 (2012).